Colloid Polym Sci 276:786–793 (1998)

ORIGINAL CONTRIBUTION

A. Flores
J. Aurrekoetxea
R. Gensler
H.H. Kausch
F.J. Baltá Calleja

Microhardness-structure correlation of iPP/EPR blends: influence of molecular weight and EPR particle content

Received: 2 February 1998
Accepted: 11 May 1998

A. Flores · F.J. Baltá Calleja (✉)
Instituto de Estructura de la Materia
CSIC, Serrano 119
28006 Madrid
Spain

J. Aurrekoetxea · R. Gensler
H.H. Kausch
Laboratoire de Polymères
EPFL, MX-D-Ecublens
1015 Lausanne
Switzerland

Abstract The influence of molecular weight on the mechanical properties of isotactic poly(propylene) (iPP) and iPP blended with ethylene-propylene copolymers has been investigated by means of the microhardness technique. The hardness (H) of iPP is shown to slightly decrease with increasing molecular mass, within the range of molecular weights investigated. The H-decrease is correlated to a loss of crystallinity as the average molecular weight increases. On annealing, the mechanical properties are enhanced as a consequence of an increase in both, the degree of crystallinity and the crystalline lamellar thickness. A value of H_c^{∞} for iPP crystals of infinite thickness in the α-form is proposed for the first time. The inclusion of EPR particles in the iPP matrix softens the material. This result could be explained in terms of an increase in the basal surface free energy of the iPP crystals with increasing amount of rubber content.

Key words Microhardness – poly(propylene) – ethylene-co-propylene rubber – blends – surface free energy

Introduction

In spite of isotactic poly(propylene) being one of the most widely investigated polymers due to its many commercial uses, there is only limited information in the literature about the influence of molecular weight on the mechanical properties of this material. The literature available concerns the tensile properties of the oriented iPP [1–3]. A comparative study of the tensile strength and elastic modulus in injection moulded iPP as compared with the self-reinforced injection moulded iPP for different molecular weights has been reported [1]. Andreassen and coworkers have recently shown that the tensile properties of iPP fibres are enhanced with increasing molecular weight as a consequence of a higher efficiency of the drawing process in producing molecular orientation [2]. Misra et al. showed that higher levels of crystallinity and orientation for melt-spun iPP filaments were obtained with increasing molecular mass [3]. Recently, the mechanical anisotropy of forged iPP has been investigated by microindentation hardness [4]. In an earlier study, we used the microhardness technique to detect the polymorphic change occurring in iPP when passing from the α to the β-form crystalline phase [5]. To our knowledge, a study of the influence of molecular mass on the microhardness of unoriented iPP is still missing. The hardness technique relies on the irreversible permanent deformation produced by a sharp indenter penetrating the specimen surface [6]. Microindentation tests are becoming widespread among the scientific community due to its simplicity and the fact that it provides valuable information about the morphology and microstructure of polymeric materials [7]. On the other hand, hardness can be related to macroscopic mechanical properties such as the yield stress [6].

In recent years, poly(propylene)/ethylene-co-propylene rubber (PP/EPR) blends have been extensively studied

[8–14]. The inclusion of EPR particles in the iPP matrix leads to a decrease of the stiffness and to an increase of the impact strength at ambient and low temperatures [8–10]. The morphology, structure, thermal behavior and mechanical properties of blends of iPP with EPR have been reported [11–13]. Kinetic and thermodynamic parameters related to the crystallization process of the iPP phase have also been investigated on melt crystallized iPP/EPR blends [14]. Modern in situ polymerized iPP/EPR reactor blends exhibit a three-phase morphology [9]. The rubber particles, which are well dispersed in the iPP matrix, display a core–shell structure. The shell is constituted by an amorphous ethylene–propylene copolymer and the core is composed by one or more lamellar polyethylene inclusions. Figure 1 shows a transmission electron micrograph (TEM) of a reactor iPP/EPR 80/20 blend investigated in our laboratory.

The aim of the present paper is two-fold: (1) to report on the microhardness variation of isotropic iPP with molecular weight. We attempt to correlate such variation with microstructural changes occurring in the crystalline and amorphous phase. (2) to examine the surface mechanical properties of iPP/EPR reactor blends with different composition and molecular mass by means of the microhardness technique.

Experimental

Materials

Four isotactic iPP samples with varying molecular weight and three iPP/EPR reactor blends with different average molecular weight and ratios were supplied by PCD Polymer (Linz, Austria) in the form of pellets. The ethylene to propylene ratio in the copolymer rubber is about 1/1. The samples were sandwiched between two plates of 15×15 cm^2 size which were subsequently introduced in the hot press. The temperature of the two-plate system was controlled using a thermocouple. Thin films 0.7 mm thick were obtained by melt pressing at 215 °C under a pressure of 50 bar and immediately cooling down at $\sim$10 °C. The rapid cooling of the samples was achieved by means of water circulating through the two-plate system. In addition, annealed samples of the iPP homopolymers were obtained by keeping the as-moulded samples for 1 h at 140 °C. Table 1 shows the weight average molecular weight, M_w, of the iPP homopolymers and the different iPP/EPR blends. In all cases, the polydispersity, M_w/M_n, is around 5.

Techniques

Calorimetric measurements were carried out using a Perkin Elmer DSC-4 differential calorimeter. The samples

Table 1 M_w for the iPP homopolymers and the iPP/EPR blends investigated

iPP/EPR	M_w [10^5 g/mol]
100/0	1.4
100/0	3.8
100/0	5.4
100/0	10.0
85/15	2.2
85/15	9.0
80/20	5.8

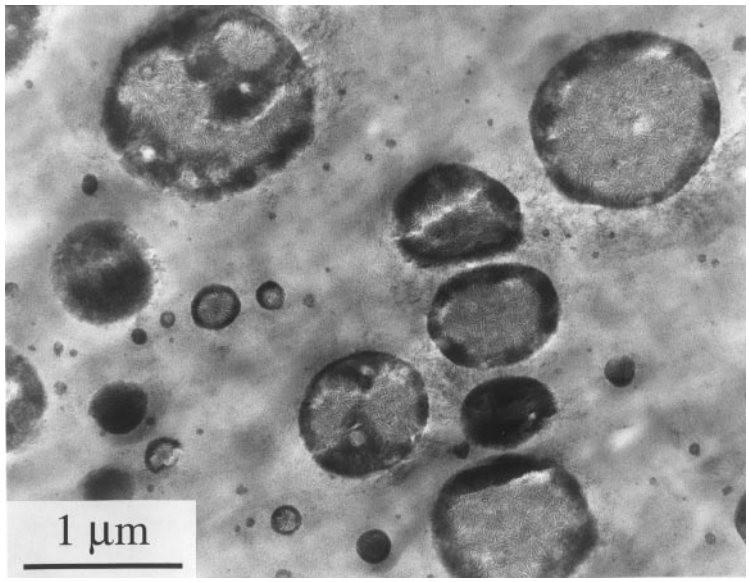

Fig. 1 TEM of a reactor iPP/EPR 80/20 blend

were heated at a rate of 10 K/min under a nitrogen flux. The heat of fusion, ΔH_f, is derived from the area under the melting peak. The weight fraction of crystalline material in the homopolymer samples, w_c, is calculated using:

$$w_c = \frac{\Delta H_f}{\Delta H_f^0}, \quad (1)$$

where ΔH_f^0 is the enthalpy of fusion of a completely crystalline isotactic PP, taken to be 207 J/g [15]. The degree of crystallinity in the blends, w_c^B, was obtained through

$$w_c^B = w_c^{PP}\phi_{PP} + w_c^{EPR}(1 - \phi_{PP}), \quad (2)$$

where w_c^{PP} and w_c^{EPR} are calculated using Eq. (1) for each of the components and ϕ_{PP} is the propylene content in the blend. The estimated standard error in the degree of crystallinity values is less than 1%. For practical reasons, ΔH_f^0 of the rubber component is approximated to that of polyethylene. This approximation is supported by the fact that transmission electron micrographs of the iPP/EPR reactor blends in Table 1 showed rubber particles having a core–shell structure as described in the introduction. In fact, the TEM of Fig. 1 corresponds to the iPP/EPR 80/20 blend of Table 1. Thus, only the PE core could exhibit crystallites. Moreover, in the DSC thermograms, no other melting peaks but that of polypropylene and a small one consistent with the melting temperature of linear polyethylene have been observed. In the following, we will denote EPR as the whole rubbery particle, including the ethylene-co-propylene shell and the PE core.

Wide-angle X-ray diffraction (WAXD) measurements were performed in a Rigaku vertical goniometer attached to a Rigaku high power X-ray generator with rotating anode (Ni-filtered CuK_α radiation) using 40 kV and 140 mA.

Small-angle X-ray diffraction (SAXD) patterns were obtained with a Kiessig camera using 40 kV and 70 mA. The long period, L, was calculated from the diffraction maximum using Bragg's law. The thickness of the crystalline lamella, l_c, was derived assuming

$$l_c = v_c L, \quad (3)$$

where v_c is the volume fraction of crystalline material, which is related to w_c through

$$v_c = \frac{\rho}{\rho_c} w_c, \quad (4)$$

ρ being the macroscopic density and ρ_c the density of the crystalline phase. The value of ρ was evaluated using

$$\frac{1}{\rho} = \frac{1 - w_c}{\rho_a} + \frac{w_c}{\rho_c}, \quad (5)$$

where ρ_a is the density of the amorphous region. $\rho_c = 0.936$ and 0.939 g/cm^3 for the α and β-form of iPP, respectively, and $\rho_a = 0.858$ g/cm^3 [16].

The l_c values obtained using Eq. (3) should be considered as a lower limit to the thickness of the iPP crystalline lamella. This is due to the possible existence of interspherulitic amorphous regions which cannot be discarded, especially in melt crystallized samples.

Microhardness technique is based on the optical measurement of the residual image left behind by a sharp indenter upon the application of a given load. Hardness, H, is defined as the applied load divided by the projected area of the impression [17]. Microindentation experiments were performed in a Leitz tester. A Vickers square-based diamond indenter was used. To minimize the creep of the sample under the indenter, a 6 s holding time was chosen. The standard error in the H values determined is $\sim$2.5%. Further details concerning the procedure are reported elsewhere [17].

Basic equations

The hardness of a semicrystalline polymer is related to the volume degree of crystallinity, v_c, and the hardness of the crystalline and the amorphous phase, H_c and H_a respectively, through [6]

$$H = v_c H_c + (1 - v_c) H_a. \quad (6)$$

This equation describes a parallel model of alternating amorphous and crystalline layers. The hardness of the amorphous PP phase can be assumed to be $H_a = 30$ MPa [18]. Using Eq. (6), values of H_c can be derived for each pair of v_c, H values.

In addition, the hardness of the crystalline phase can be described by [19]

$$H_c = \frac{H_c^\infty}{1 + (b/l_c)} \quad (7)$$

where H_c^∞ is the hardness of an infinitely thick crystal and b is a parameter related to the surface free energy σ_e of the crystals and to the energy Δh required for plastic deformation of the crystals. The parameter b is equal to $2\sigma_e/\Delta h$.

Microhardness of a polymer blend can be described in terms of an additive system of two independent components [6]

$$H = H_1\phi + H_2(1 - \phi), \quad (8)$$

where H_1 and H_2 are the hardness of the single components and ϕ is the weight fraction of component 1. However, deviations from Eq. (8) may occur. In PP/PE blends, the presence of molten PE within the blend has shown to

notably affect the crystallization behaviour of the PP phase [17]. In this case, Eq. (8) may be rewritten as

$$H = [v_c^{PP} H_c^{PP} + (1 - v_c^{PP}) H_a^{PP}] \phi_{PP} + [v_c^{PE} H_c^{PE} + (1 - v_c^{PE})\, H_a^{PE}](1 - \phi_{PP}) , \quad (9)$$

in which the variation of crystallinity of each phase and H_c^{PP} and H_c^{PE} can be taken into account.

Results and discussion

Homopolymers: influence of molecular weight

Wide-angle X-ray diffraction patterns of quenched iPP samples with $M_w = 3.8 \times 10^5$ and 10^6 g/mol are shown in Fig. 2A and B, respectively. The diffraction maxima in Fig. 2A are consistent with the monoclinic α-form of isotactic poly(propylene) [1]. The X-ray profile in Fig. 2B shows an additional small diffraction peak at $2\theta = 16.2^\circ$, which is associated to the hexagonal β-form of iPP [1]. In all other samples investigated, only the α-form contributed to the X-ray diffraction pattern. The simultaneous formation of the α and the β-form has been observed at high supercoolings [1]. In addition, Varga and colleagues found that high molecular weight iPP was more susceptible to β-crystallization [1]. From all the samples investigated in the present paper, only the iPP sample with the highest molecular mass and crystallized at high supercooling with no further thermal treatment, revealed the presence of an appreciable amount of crystallites in the β-form.

Figure 3 shows the dependence of the degree of crystallinity values as measured from DSC experiments, upon molecular weight for the series of quenched and annealed iPP samples. A clear w_c decrease M_w is observed in the samples quenched from the melt. Annealed samples show higher w_c values than samples quenched from the melt together with a smaller tendency of w_c to diminish as M_w increases.

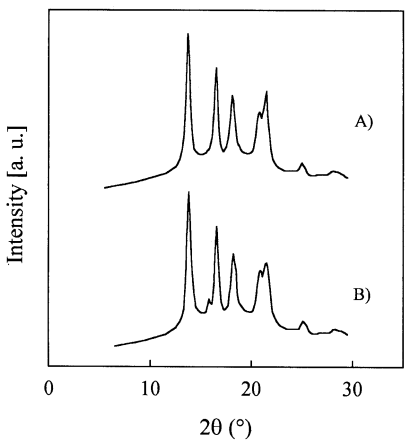

Fig. 2 WAXS diffractograms of quenched iPP samples with a M_w of: (A) 3.8×10^5 g/mol; (B) 10^6 g/mol

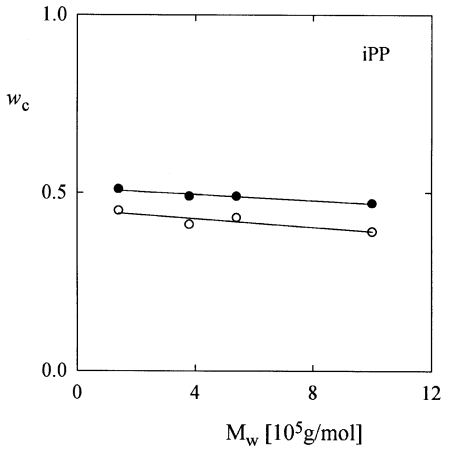

Fig. 3 Plot of degree of crystallinity as a function of molecular mass for quenched (open symbols) and annealed (solid symbols) iPP samples

Table 2 Long spacing and crystalline lamellar thickness for quenched and annealed iPP samples with different M_w

M_w [10^5 g/mol]	Quenched samples		Annealed samples	
	L [Å]	l_c [Å]	L [Å]	l_c [Å]
1.4	128	55	176	86
3.8	150	59	192	90
5.4	146	60	198	93
10.0	172	64	220	99

Table 2 shows the values of the long period and the minimum crystalline lamellar thickness values for the iPP samples with different molecular weights. Both, quenched and annealed samples, show a clear L increase with M_w which seems to be partly due to a l_c thickening as M_w increases. However, one cannot discard that the l_c value may remain constant with M_w. This would mean that the w_c-decrease with increasing M_w observed (see Fig. 3) is partly due to an increasing amount of amorphous interspherulitic material with M_w. In any case, the amorphous layer ($l_a = L - l_c$) also contributes to the L increase with M_w. This effect could be accounted for by assuming a higher concentration of chain entanglements in the melt as the molecular weight of the sample is increased. During crystallization, such defects tend to segregate between crystals contributing to the thickening of the amorphous layer [20, 21].

On annealing, an increase in the long spacing is observed (see Table 2). It is reasonable to expect a thickening of the crystalline lamellae upon annealing [22].

H and H_c values of quenched and annealed iPP samples are plotted in Fig. 4 as a function of M_w. The H_c constancy and the slight H decrease with molecular mass observed for iPP are similar to the behavior reported for quenched and slowly cooled from the melt PE samples in same M_w interval [21]. Figure 4 shows a remarkably low H_c value of 160 MPa for the iPP homopolymer with $M_w = 10^6$ g/mol (quenched series). This is due to the presence of crystallites in the β-form which are known to exhibit lower H_c values [5]. On annealing, the hexagonal β-form is transformed into the monoclinic α-form as revealed by the disappearance of the diffraction maximum at $2\theta = 16.2^\circ$. This transformation leads to a conspicuous increase of H_c up to 214 MPa. In addition, all the annealed samples show higher H_c values ($H_c \sim 211$ MPa) with respect to those of the quenched samples ($H_c \sim 202$ MPa). H_c is known to depend on l_c through Eq. (7). Thus, the observed H_c increase upon annealing confirms that a thickening of the lamellae takes place when the samples are annealed at high temperature. Neither the quenched samples with crystallites in the α-form, nor the annealed series show a H_c variation with M_w (Fig. 4 top). At the same time, the crystalline lamellar thickness increases by 15% at most over the M_w range investigated (see Table 2). This l_c variation (if any) is not sufficient to contribute to a sensitive H_c variation with molecular mass.

H is related to H_c through Eq. (6). In our case, the second term of Eq. (6) contributes by less than 18% to H. Hence, the hardness behavior of the series of iPP samples with different molecular weights is essentially due to the value of H_c modulated by w_c, which shows a decreasing tendency with increasing M_w.

Fig. 4 Plot of H and H_c as a function of M_w for quenched (open symbols) and annealed (solid symbols) iPP samples. The β symbol refers to the sample where the α and β-form coexist

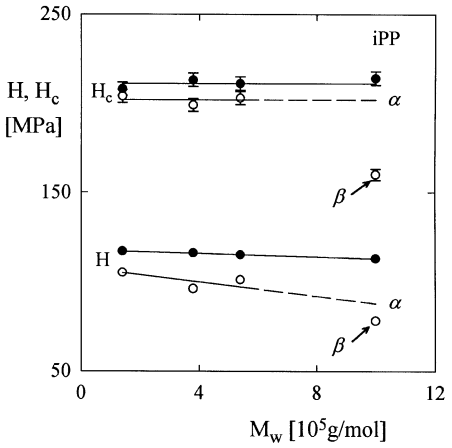

Blends: influence of rubber content

WAXD experiments on quenched iPP/EPR samples show a diffraction pattern consistent with the α-form of iPP.

Table 3 collects the values of the weight fraction of crystallinity for each one of the components of the blend, w_c^{PP} and w_c^{EPR}, calculated using Eq. (1) and the total degree of crystallinity in the blends, w_c^B, obtained using Eq. (2) as a function of EPR content in the blend (ϕ_{EPR}) and M_w of the samples. Table 3 shows an increase in the crystallinity of iPP within the blends with respect to the values of pure isotactic PP (see Fig. 3). This result could be explained in terms of Greco and colleagues' finding who observed that EPR acts as a nucleating agent in iPP/EPR blends [11]. On the other hand, the EPR component possess a very low degree of crystallinity (<2%). The EPR's negligible contribution to the overall crystallinity counterbalances the enhanced degree of crystallinity in the iPP phase, yielding w_c values of the blends which are comparable to those determined for the homopolymers. Figure 5 shows the variation of w_c vs. M_w for iPP samples with different EPR content. The w_c values for the homopolymers are included for comparison. The decreasing tendency of the crystallinity with increasing M_w observed in the homopolymers is also found for the iPP/EPR blends.

Table 4 shows the long spacing and the crystalline lamellar thickness for all the iPP/EPR blends investigated. L and l_c are always referred to iPP crystals as no coherent diffraction corresponding to the rubber particles due to their low crystallinity was detected. Contrary to what we observe in the case of the homopolymers, L appears to be nearly constant with M_w.

Figure 6 illustrates the hardness of iPP/EPR blends for various molecular weight values. H values of the pure isotatic PP samples in the α-form have been included for comparison. To calculate the hardness of the iPP crystalline phase within the blends, Eq. (8) describing the

Table 3 Weight fraction crystallinity of the iPP and EPR component, w_c^{PP} and w_c^{EPR}, respectively, and overall crystallinity in the blend, w_c^B, for the iPP/EPR samples with different blend ratio and molecular mass

M_w [10^5 g/mol]	ϕ_{EPR} [%]	w_c^B	w_c^{PP}	w_c^{EPR}
2.2	15	0.45	0.53	0.02
5.8	20	0.43	0.54	0.01
9.0	15	0.38	0.45	0.004

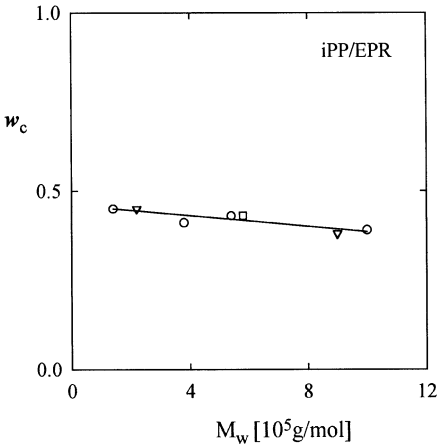

Fig. 5 Variation of the degree of crystallinity for the iPP/EPR blends containing different EPR content as a function of molecular weight. ▽: iPP/EPR 85/15; □: iPP/EPR 80/20. Values for the iPP homopolymers (○) are included for comparison

Table 4 L and l_c for the iPP/EPR blends investigated

iPP/EPR	M_w [10^5 g/mol]	L [Å]	l_c [Å]
85/15	2.2	124	63
80/20	5.8	126	66
85/15	9.0	128	55

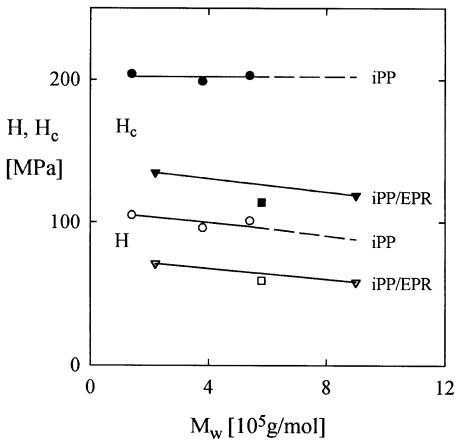

Fig. 6 Molecular weight dependence of H (open symbols) and H_c (solid symbols) for the different quenched samples investigated. ▽, ▼: iPP/EPR 85/15; □, ■: iPP/EPR 80/20; ○, ●: iPP

hardness in a two-component blend was used. In our case, $v_c^{EPR} \sim 0$. The hardness of the amorphous EPR phase can be approximated to that of polyethylene, i.e. $H_a^{PE} \sim 0$, as it is measured above its glass transition temperature [23]. Hence, the hardness of the crystalline phase of the iPP crystals is related to the hardness of the blends through

$$H = [v_c^{PP} H_c^{PP} + (1 - v_c^{PP}) H_a^{PP}] \phi_{PP} \quad (1)$$

H_c^{PP} values calculated using this equation are included in Fig. 6. Values of v_c^{PP} are obtained through Eq. (4) (w_c^{PP} values are taken from Table 3). H_a^{PP} was taken equal to 30 MPa as previously reported. The first finding is that H_c values of iPP in the blends are appreciably smaller than H_c in the homopolymers. Figure 6 shows that H_c for the blends slightly decreases with molecular weight. H_c also seems to decrease with the rubber content in the blend. For the 85/15 blend, l_c decreases $\sim 13\%$ over the M_w range investigated (see Table 4). It is very unlikely that this small l_c variation would produce such a remarkable change in the H_c values. The H_c decrease with increasing M_w observed for the 85/15 blend could, most probably, be assigned to a change in the b parameter. This issue will be further discussed in the next section. The hardness variation with M_w shows a parallelism with the H_c and crystallinity trend to decrease as M_w increases (see Fig. 5). The smaller H values of the blends with respect to the homopolymers are the result of a smaller H_c.

Figure 7 shows the notorious H decrease obtained as a function of the EPR content. The data correspond to samples of similar M_w ($\sim 5.5 \times 10^5$ g/mol). The H value for the iPP/EPR 85/15 blend at this molecular mass was calculated by interpolation (see Fig. 6). The straight line describes the hardness of an additive system of two independent components (Eq. (8)). The deviation of the hardness values corresponding to 15 and 20% EPR from the hardness additivity law is a consequence of the lower H_c values found.

Fig. 7 Plot of hardness as a function of the EPR content in the blends. The straight line corresponds to the hardness of the additivity law (Eq. (8))

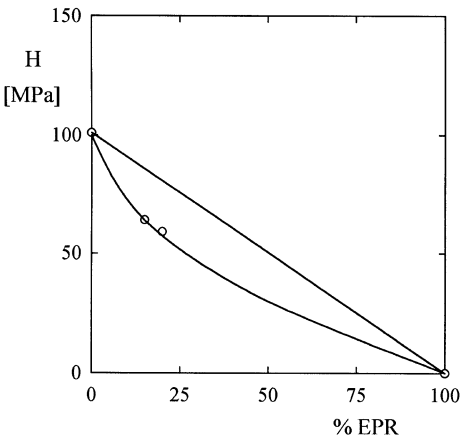

Microhardness of infinitely large iPP crystals

If we plot $1/H_c$ vs. $1/l_c$ (see Fig. 8), according to Eq. (7) we obtain a value of $H_c^\infty = 230$ MPa for the microhardness of infinitely thick iPP crystals. This value is substantially larger than that found for PE [19] ($H_c^\infty = 170$ MPa). The result is in agreement with the higher equilibrium melting point, T_m^o, of iPP in contrast to PET [24]. The b value obtained from the plot of Fig. 8 for iPP is equal to $b \sim 8$ Å. This is derived using $l_c = v_c L$, which is evidently a lower bound. If we assume $l_c \sim L$, then $b \sim 22$ Å and H_c^∞ remains approximately the same. The real b value will lie between 8 and 22 Å, which is comparable to the ratio $b' = 2\sigma_e/\Delta h_f \sim 10$ Å derived from the melting point depression, where $\Delta h_f \sim 2.07 \times 10^9$ erg/cm^3 is the heat fusion of the crystals [15] and $\sigma_e \sim 10^2$ erg/cm^2 is the fold surface free energy [1, 24]. It turns out that the enthalpy involved during plastic deformation under the indenter is nearly the same than the enthalpy required to melt the crystals, in contrast to what was found before for PE [20]. This finding would suggest that plastic deformation of iPP homopolymer involves a local melting of crystals.

The b values for the iPP crystals in the blends were obtained assuming the same H_c^∞ value as that for the homopolymers. Figure 8 shows that the three different blends do not fit in the same linear regression. On the contrary, a straight line has to be drawn for each sample, thus, leading to various b values. The lowest b value (=44 Å) corresponds to the iPP/EPR blend with the lowest M_w and rubber content. This value is much higher than the b value obtained for the homopolymer. The highest b value (=67 Å) found corresponds to the 80/20 polymer blend which is known to possess the highest EPR content. Thus, it seems that b increases with increasing amount of rubber content and M_w of the blend. This might be the result of an increase of the surface free energy due to the occurrence of more defects at the surface of the crystals surrounding the EPR particles.

Hardness to yield stress correlation

As mentioned in the introduction, hardness is related to the yield stress, σ_y. According to the theory of plasticity, the hardness value for a Vickers indenter is approximately equal to three times the yield stress in frictionless compression [25]. Baltá Calleja showed that, for a wide variety of semicrystalline polyethylene samples, the H/σ_y ratio was close to 3, σ_y being the yield stress in tension [26]. Smaller values for the H/σ_y ratio are obtained when the strain rate of the tensile test is much larger than that used in the indentation test [26]. Values smaller than $H/\sigma_y = 3$ were also found when using the yield stress in compression [27]. In order to investigate the $H - \sigma_y$ correlation, yield stress values of the iPP homopolymers and the iPP/EPR blends investigated in this paper were obtained using a conventional tensile equipment [28]. The tensile experiments were carried out using a crosshead speed of 10 mm/min. Figure 9 shows the plot of H vs. σ_y values for all the samples investigated. The H, σ_y values for the iPP homopolymer with the lowest molecular mass are not included in Fig. 9 as this material showed no yield drop. A first-order regression passing through the origin to the data in Fig. 9 (quenched samples) gives a slope

Fig. 8 Plot of H_c^{-1} vs. l_c^{-1} for iPP homopolymers and iPP/EPR blends. ▽: iPP/EPR 85/15; □: iPP/EPR 80/20; ○: quenched iPP; ●: annealed iPP

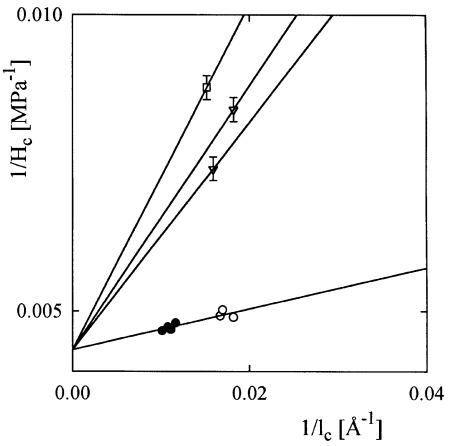

Fig. 9 Plot of H vs. σ_y for the different iPP homopolymers and iPP/EPR blends. Symbols as in Fig. 5

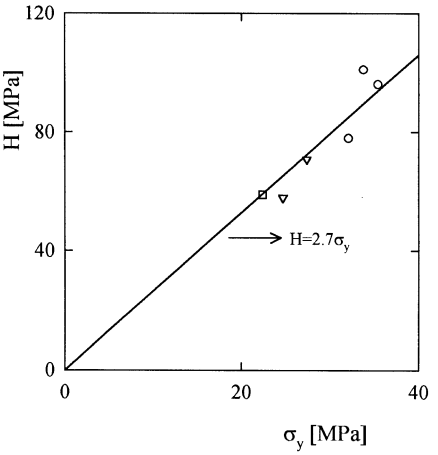

of 2.7, which is consistent with the above mentioned results.

Conclusions

iPP homopolymers

- Microhardness of iPP slightly diminishes with M_w as a consequence of a decrease in the degree of crystallinity as molecular mass increases.
- The low H value found for the highest iPP molecular weight sample ($M_w \sim 10^6$ g/mol) is due to the presence of β-phase crystallites.
- Upon annealing, microhardness increases owing to an increase of both, l_c and w_c.
- The hardness of the crystalline phase (α-form) is constant over the M_w range investigated for both, the quenched and the annealed samples. The small l_c increase along the M_w range considered, is not sufficient to produce an appreciable H_c variation.
- The hardness of an infinitely thick iPP crystal in the α-form has been calculated to be 230 MPa.

iPP/EPR blends

- The inclusion of EPR particles in the iPP matrix lowers the hardness values by 30–40%. This H decrease is due to a smaller H_c value in the blends with respect to that in the homopolymers.
- The hardness of the iPP/EPR blends tendency to diminish with M_w can be explained in terms of a H_c and w_c decrease with M_w.
- The microhardness of the iPP/EPR blends deviate from that corresponding to an additive system of two independent components ($H^{PP} = 100$ MPa; $H^{EPR} = 0$ MPa). The deviations from this additivity law are attributed to the lower H_c values of the iPP crystals found in the blends in contrast to those of the homopolymers. This finding is directly related to the fact that the b-parameter seems to increase with increasing amount of rubber content and molecular mass of the blend.

Acknowledgements We are endeavoured to Dr. W. Neissl (PCD Polymer, Linz, Austria) for kindly providing the investigated materials and molecular weight data. Grateful acknowledgement is due to Dirección General de Investigación Científica y Técnica (DGICYT), Spain, for support of this investigation (Grant PB94-0049).

References

1. Karger-Kocsis J (ed) (1995) Polypropylene: Structure, blends and composites, Vol 1. Chapman & Hall, London
2. Andreassen E, Myhre OJ, Hinrichsen EL, Grøstad K (1994) J Appl Polym Sci 52:1505
3. Misra S, Lu FM, Spruiell JE, Richeson GC (1995) J Appl Polym Sci 56:1761
4. Osawa S, Porter RS (1996) Polymer 37: 2095
5. Baltá Calleja FJ, Martínez Salazar J, Asano T (1988) J Mater Sci Lett 7:165
6. Baltá Calleja FJ (1994) Trends Polym Sci 2:419
7. Baltá Calleja FJ, Fakirov S (1997) Trends Polym Sci 5:246
8. D'Orazio L, Mancarella C, Martuscelli E, Polato F (1991) Polymer 32:1186
9. Kim GM, Michler GH, Gahleitner M, Fiebig J (1996) J Appl Polym Sci 60:1391
10. Mirabella Jr FM (1993) Polymer 34:1729
11. Greco R, Mancarella C, Martuscelli E, Ragosta G, Jinghua Y (1987) Polymer 28:1929
12. Coppola F, Greco R, Martuscelli E, Kammer HW, Kummerlowe C (1987) Polymer 28:47
13. Greco R, Martuscelli E, Ragosta G, Jinghua Y (1988) J Mater Sci 23:4307
14. D'Orazio L, Mancarella C, Martuscelli E, Sticotti G (1991) J Mater Sci 26:4033
15. Bu HS, Cheng SZD, Wunderlich B (1988) Makromol Chem Rapid Commun 9:76
16. Samuels RJ (1965) J Polym Sci (A) 3:1741
17. Baltá Calleja FJ (1985) Adv Polym Sci 66:117
18. Martínez Salazar J, García Tijero JM, Baltá Calleja FJ (1988) J Mater Sci 23:862
19. Baltá Calleja FJ, Kilian HG (1985) Colloid Polym Sci 263:697
20. Baltá Calleja FJ, Santa Cruz C, Bayer RK, Kilian HG (1990) Colloid Polym Sci 268:440
21. Bayer RK, Baltá Calleja FJ, Kilian HG (1997) Colloid Polym Sci 275:432
22. Baltá Calleja FJ, Peterlin A (1971) Makromol Chem 141:91
23. Baltá Calleja FJ, Kilian HG (1988) Colloid Polym Sci 266:29
24. Wunderlich B (1980) Macromolecular Physics, Vol 3. Academic Press, New York
25. Tabor D (1951) The Hardness of Metals. Oxford University Press, London
26. Baltá Calleja FJ, Giri L, Ward IM, Cansfield DLM (1995) J Mater Sci 30:1139
27. Baltá Calleja FJ, Attenburrow GF, Basset DC (unpublished results)
28. Gensler R (unpublished results, Lausanne 1997)